Statistical theory of light-nucleus reactions and application to the ^{9}Be(p,xn) reaction

Xiaojun Sun*
College of Physics, Guangxi Normal University, Guilin 541004, People's Republic of China
and State Key Laboratory of Theoretical Physics, Institute of Theoretical Physics, Chinese Academy of Sciences, Beijing 100190, People's Republic of China

Jingshang Zhang
China Institute of Atomic Energy, P.O. Box 275(41), Beijing 102413, People's Republic of China
(Received 23 October 2015; published 11 January 2016)

A statistical theory of light nucleus reactions (STLN) is proposed to describe both neutron and light charged particle induced nuclear reactions with 1p-shell light nuclei involved. The dynamics of STLN is described by the unified Hauser-Feshbach and exciton model, in which the angular momentum and parity conservations are strictly considered in equilibrium and pre-equilibrium processes. The Coulomb barriers of the incoming and outgoing charged particles, which significantly influence the open channels of the reaction, can be reasonably considered in the incident channel and different outgoing channels. In kinematics, the recoiling effects in various emission processes are strictly taken into account. The analytical double-differential cross sections of the reaction products in sequential and simultaneous emission processes are obtained in terms of the new integral formula proposed in our recent paper [Phys. Rev. C **92**, 061601(R) (2015)]. Taking the ^{9}Be(p,xn) reaction as an example, we calculate the double-differential cross sections of outgoing neutrons and charged particles using the PUNF code in the frame of STLN. The existing experimental double-differential cross sections of neutrons at $E_p = 18$ MeV can be remarkably well reproduced, which indicates that the PUNF code is a powerful tool to set up "file-6" in the reaction data library for light charged particle induced nuclear reactions with 1p-shell light nuclei involved.

DOI: 10.1103/PhysRevC.93.014609

I. INTRODUCTION

The 1p-shell light elements (Li, Be, B, C, N, and O) had long been selected as the most important materials for improving neutron economy in thermal and fast fission reactors and in the design of accelerator-driven spallation neutron sources, with uses such as a candidate for target material in the intense neutron source of the International Fusion Materials Irradiation Facility (IFMIF) [1], the plasma facing material of the first wall in the International Thermonuclear Experimental Reactor (ITER) [2], the neutron multiplier in fusion blankets [3], the neutron protection layer of the Molten Salt Fast Reactor (MSFR) [4], the material of the accelerator-based neutron source in the Fixed Field Alternating Gradient (FFAG) accelerator [5], and the Accelerator Driven Advanced Nuclear Energy System (ADANES) [6]. Additionally, some 1p-shell light elements are the materials used in the determination of radiation shielding requirements for radiation protection purposes, optimization of dose delivery to a treatment volume, decisions on biological effectiveness of different therapy beams, and so on [7]. For the accurate designs of target systems, neutron shielding, and nuclear medicine, the double-differential cross sections of the reaction products are very important as a source term for light particle (including neutron and light charged particles) induced nuclear reactions with 1p-shell light nuclei involved.

For neutron induced nuclear reactions with 1p-shell light nuclei involved, the model calculations of the double-differential cross sections of reaction products have been successfully performed [8]. "File-6" was established in the CNDEL-3.1 library based on theoretical calculations below 20 MeV incident energy [9]. File-6 is one of the most important files of the nuclear reaction database, and is recommended when the energy and angular distributions of the emitted particles must be coupled, when it is important to give a concurrent description of neutron scattering and particle emission, when so many reaction channels are open that it is difficult to provide separate reactions, or when accurate charged particle or residual nucleus distributions are required for particle transport, heat deposition, or radiation damage calculations [10].

However, the double-differential cross sections of reaction products for light charged particle induced nuclear reactions with 1p-shell light nuclei involved are scarce, especially below 20 MeV incident energies. For example, in the case of the $p + {}^{9}$Be reaction, there are some coarse double-differential cross sections of reaction products only in ENDF/B-VII.1 [11] and TENDL-2012 [12]. Only some double-differential cross sections of outgoing neutrons have been measured at several incident energies, and several peaks are observed for the ^{9}Be(p,xn) reaction. These peaks come mainly from the transitions between the discrete energy levels of the residual nuclei. The neutron double-differential cross sections of ENDF/B-VII.1, obtained by the Intranuclear Cascade Evaporation (ICE) model [13], cannot appropriately reproduce these experimental peaks (including positions and quantities), although the ICE model is most applicable to a few hundreds MeV incident energies. The results of TENDL-2012 calculated by the code TALYS [14] also cannot reasonably well reproduce the double-differential cross sections for the ^{9}Be(p,xn) reaction. In

*sxj0212@gxnu.edu.cn

addition, Monte Carlo calculation using the Particle and Heavy Ion Transport System (PHITS) code is performed by a method combining the evaluated nuclear data files of ENDF/B-VII, the Bertini/GEM model, and the JQMD/GEM model [15]. The calculated results cannot reproduce very well the experimental double-differential cross sections for the ^{9}Be(p,xn) reaction at 10 MeV incident energy. Recently, Hashimoto *et al.* proposed a nuclear reaction model that is a combination of the intranuclear cascade model and the distorted wave Born approximation to estimate neutron spectra of proton induced Li and Be reactions using the PHITS code [16]. But there are some divergences between the calculated results and experimental double-differential cross sections for the ^{9}Be(p,xn) reaction at 39 MeV with 0 angle.

In addition, the continuum discretized coupled channels (CDCC) method is used to calculate the double-differential cross sections both for neutron and proton induced ^{6,7}Li reactions, but it cannot be applied to the sequentially secondary particle emission processes [17–20]. Apart from the theoretical studies, to our knowledge there are no published double-differential cross sections for light charged particle induced reactions with the 1p-shell nuclei involved.

Although much effort has been made during the past several decades, there is a lack of the appropriate theories or methods that can satisfactorily reproduce the measured double-differential cross sections for light charged particle induced nuclear reactions with the 1p-shell light nuclei involved. This problem may originate from several sources. First, there is no theoretical method to describe the particle emission processes between the discrete levels of the residual nuclei with a pre-equilibrium mechanism, which dominates all of the 1p-shell light nucleus reactions. Second, because of light mass, the recoil effect of the energy conservation must be strictly taken into account. Furthermore, there are individual features of each energy level (including energy, spin, parity, width, branching ratio, and so on) for each 1p-shell light nucleus. In this paper, the statistical theory of light nucleus reactions (STLN), which can describe the sequential and simultaneous particle emission processes between the discrete levels, keeping conservations of energy, angular momentum, and parity, is proposed to calculate the double-differential cross sections of outgoing neutrons and charged particles both for neutron and light charged particle induced reactions with the 1p-shell nuclei involved. Simultaneously, taking the ^{9}Be(p,xn) reaction at 18 MeV as an example, we calculate the double-differential cross sections of outgoing neutrons first using the PUNF code in the frame of STLN. The calculated results are in good agreement with the existing experimental data.

The structure of this paper is as follow. In Sec. II, the dynamics and kinematics of STLN are introduced in detail. The reaction channels of the p + ^{9}Be reaction are analyzed, and the calculated results are compared with the experimental data in Sec. III. In Sec. IV, a summary is given.

II. STATISTICAL THEORY OF LIGHT NUCLEUS REACTION

It is assumed that the pre-equilibrium emission process from a compound nucleus to discrete levels of the residual nuclei plays a dominant role in light particle induced light nucleus reactions. Thus the dynamics of STLN can be described by the unified Hauser-Feshbach and exciton model [21–23], which has been applied successfully to calculate the double-differential cross sections of outgoing neutrons for neutron induced ^{6}Li [24], ^{7}Li [25], ^{9}Be [26,27], ^{10}B [28], ^{11}B [29], ^{12}C [7,30,31], ^{14}N [32], ^{16}O [33,34], and ^{19}F [35] reactions.

To conveniently describe the dynamics and kinematics, some quantities are defined as follows:

M_T: mass of the target nucleus with mass number A_T, proton number Z_T, and neutron number N_T;
E_L: kinetic energy of the incident particle in the laboratory system;
m_0: mass of the incident particle with mass number A_0, proton number Z_0, and neutron number N_0;
M_C: mass of the compound nucleus with mass number $A_C = A_T + A_0$ and excited energy $E^* = \frac{M_T}{M_C}E_L + B_0$;
m_1 and M_1: masses of the first emitted particle and its residual nucleus, respectively;
m_2 and M_2: masses of the secondary particle emitted from M_1 and its residual nucleus, respectively;
B_0, B_1, and B_2: binding energies of m_0, m_1 in M_C, and m_2 in M_1, respectively;
$\varepsilon^X_{m_1}$ and $E^X_{M_1}$: kinetic energies of m_1 and M_1 in the X coordinate system, respectively;
$\varepsilon^X_{m_2}$ and $E^X_{M_2}$: kinetic energies of m_2 and M_2 in the X coordinate system, respectively.

Here, three motion systems will be used in STLN. Superscripts ($X = l,c,r$) denote the laboratory system (LS), the center-of-mass system (CMS), and the recoil nucleus system (RNS), respectively. For convenience, masses m_i (i = 0,1,2) and M_i (i = 1,2,T,C) defined above also indicate the corresponding particle or nucleus. It is obvious that there are approximate relations without lowering precision, i.e., $M_C \approx m_0 + M_T \approx m_1 + M_1$ and $M_1 \approx m_2 + M_2$.

A. Dynamics

1. First particle emission process

In the frame of STLN, the cross section of the first emitted particle m_1 with kinetic energy $\varepsilon^c_{m_1}$ from compound nucleus M_C to the k_1th discrete energy level of residual nuclei M_1 can be described as [23]

$$\sigma_{m_1,k_1}(E_L) = \sum_{j\pi}\sigma_a^{j\pi}(E_L)\left\{\sum_{n=3}^{n_{\max}}P^{j\pi}(n)\frac{W^{j\pi}_{m_1,k_1}\left(n,E^*,\varepsilon^c_{m_1}\right)}{W_T^{j\pi}(n,E^*)} + Q^{j\pi}(n)\frac{W^{j\pi}_{m_1,k_1}\left(E^*,\varepsilon^c_{m_1}\right)}{W_T^{j\pi}(E^*)}\right\}, \quad (1)$$

where $P^{j\pi}(n)$ is the occupation probability of the nth exciton state in the $j\pi$ channel (j and π denote the angular momentum and parity in the final state, respectively). $P^{j\pi}(n)$ can be obtained by solving the j-dependent exciton master equation under the conservation of angular momentum in pre-equilibrium reaction processes. $Q^{j\pi}(n)$ is the occupation probability of the equilibrium state in the $j\pi$ channel,

expressed as

$$Q^{j\pi}(n) = 1 - \sum_{n=3}^{n_{\max}} P^{j\pi}(n). \tag{2}$$

The absorption cross section $\sigma_a^{j\pi}(E_L)$ in the $j\pi$ channel can be derived by Hauser-Feshbach statistical theory as [36]

$$\sigma_a^{j\pi}(E_L) = \frac{\pi}{k^2}\frac{(2j+1)}{(2I_T+1)(2s_0+1)} \times \sum_{S=|I_T-s_0|}^{I_T+s_0} \sum_{l=|j-S|}^{\min\{j+S,l_{\max}\}} T_l\left(\varepsilon_{m_1}^c\right) g_l(\pi,\pi_T), \tag{3}$$

where I_T,π_T are the spin and parity of the target M_T, respectively. s_0 is the spin of incident particle m_0, and k is the incident wave vector. $T_l(\varepsilon_{m_1}^c)$ is the reduced penetration factor of the first emitted particle m_1 [37], which can be obtained by the optical model of the spherical nucleus including the Coulomb barrier of the incident charged particle.

In addition, parity conservation is determined by the orbit angular momentum l of the relative motion between the incident particle m_0 and target nucleus M_T in incident channel. For describing the parity conservation, we define the function

$$g_l(\pi,\pi_T) = \begin{cases} 1 & \text{if } \pi = (-1)^l\pi_T, \\ 0 & \text{if } \pi \neq (-1)^l\pi_T, \end{cases} \tag{4}$$

where π and π_T are the parities of the compound nucleus M_C and the target nucleus M_T, respectively.

The emission rate $W_{m_1,k_1}^{j\pi}(n,E^*,\varepsilon_{m_1}^c)$ of the first emitted particle m_1 in Eq. (1) at the nth exciton state with outgoing kinetic energy $\varepsilon_{m_1}^c$ can be expressed as

$$W_{m_1,k_1}^{j\pi}\left(n,E^*,\varepsilon_{m_1}^c\right) = \frac{1}{2\pi\hbar\omega^{j\pi}(n,E^*)} \sum_{S=|j_{k_1}-s_{m_1}|}^{j_{k_1}+s_{m_1}} \sum_{l=|j-S|}^{j+S} T_l\left(\varepsilon_{m_1}^c\right) g_l(\pi,\pi_{k_1}) F_{m_1[\lambda,m]}\left(\varepsilon_{m_1}^c\right) Q_{m_1}(n)_{[\lambda,m]}, \tag{5}$$

where $\omega^{j\pi}(n,E^*)$ is the nth exciton state density. j_{k_1} is the angular momentum of the residual nucleus M_1 at energy level E_{k_1}, and s_{m_1} is the spin of the first emitted particle m_1. π and π_{k_1} are the parities of the compound M_C and residual nuclei M_1 at energy level E_{k_1}, respectively. The functions of parity conservation are expressed as Eq. (4), only substituting the parity π_T of the target nucleus with the parity π_{k_1} of the residual nucleus at the k_1 energy level.

In the exciton model, p and h denote the particle number and hole number at the nth exciton state ($n = p + h$), respectively. $Q_{m_1}(n)_{[\lambda,m]}$, considering the effect of the incident particle memories, is the combination factor of the n th exciton state expressed as [38]

$$Q_{m_1}(p,h)_{[\lambda,m]} = \left(\frac{A_T}{Z_T}\right)^{Z_{m_1}}\left(\frac{A_T}{N_T}\right)^{N_{m_1}}\binom{p}{\lambda}^{-1}\binom{A_T-h}{m}^{-1}\binom{A_{m_1}}{Z_{m_1}}^{-1}\sum_{i=0}^{h}\binom{h}{i}\left(\frac{Z_T}{A_T}\right)^{i}\left(\frac{N_T}{A_T}\right)^{h-i} \times \sum_{j}\binom{Z_{m_1}+i}{j}\binom{N_{m_1}+h-i}{\lambda-j}\binom{Z-i}{Z_{m_1}-j}\binom{N-h+i}{N_{m_1}-\lambda+j}, \tag{6}$$

where A_{m_1}, Z_{m_1}, and N_{m_1} are the mass number, proton number, and neutron number of the first emitted particle m_1, respectively. $A_{m_1} = \lambda + m$ denotes that there are λ nucleons above the Fermi sea and m nucleons blow the Fermi sea for the emitted particle m_1. The notation $\binom{n}{m}$ is the binomial coefficient.

If the first emitted particle m_1 is a nucleon, the result is $\lambda = 1, m = 0$. Especially, if m_1 is a neutron, i.e., $A_{m_1} = N_{m_1} = 1$ and $Z_{m_1} = 0$, then Eq. (6) can be simplified as [39]

$$Q_n(p,h)_{[1,0]} = \left(\frac{A_T}{N_T}\right)\frac{1}{p}\sum_{i=0}^{h}\binom{h}{i}\left(\frac{Z_T}{A_T}\right)^{i}\left(\frac{N_T}{A_T}\right)^{h-i} \times \left(N_{m_1}+h-i\right). \tag{7}$$

Similarly, if m_1 is a proton, i.e., $A_{m_1} = Z_{m_1} = 1$ and $N_{m_1} = 0$, Eq. (6) can be also simplified as [39]

$$Q_p(p,h)_{[1,0]} = \left(\frac{A_T}{Z_T}\right)\frac{1}{p}\sum_{i=0}^{h}\binom{h}{i}\left(\frac{Z_T}{A_T}\right)^{i}\left(\frac{N_T}{A_T}\right)^{h-i}\left(Z_{m_1}+i\right). \tag{8}$$

Obviously, if m_1 is a γ photon, i.e., $A_{m_1} = Z_{m_1} = N_{m_1} = 0$, Eq. (6) can be best simplified as $Q_\gamma(p,h)_{[0,0]} = 1$. Apparently, the combination factor strictly keeps the particle conservation, i.e.,

$$\frac{N_T}{A_T}Q_n(p,h)_{[1,0]} + \frac{Z_T}{A_T}Q_p(p,h)_{[1,0]} = 1. \tag{9}$$

In Eq. (5), $F_{m_1[\lambda,m]}(\varepsilon_{m_1}^c)$ is the the pre-formation probability of composite particles m_1 at the nth exciton state in compound nucleus M_C, in which the momentum distributions of the exciton states are taken into account [40]. The consideration of the momentum distribution, which can improve the Iwamoto-Harada model with no restriction in the momentum space, enhances the pre-formation probability of the $[1,m]$ configuration and suppresses that of the $[l > 1,m]$ configurations significantly.

Considering the energy-momentum conservation in the center-of-mass system (CMS), the definitive kinetic energies of the first emitted particle m_1 can be easily derived as

$$\varepsilon_{m_1}^c = \frac{M_1}{M_C}\left(E^* - B_1 - E_{k_1}\right). \tag{10}$$

However, if the emitted particle m_1 is a charged particle, there is a threshold energy $E_{\min}^{m_1}$ because of the Coulomb barrier $V_{\rm Coul} \approx \frac{e^2 Z_{m_1} Z_{M_1}}{R_c}$ $[R_c \approx r_c(A_{m_1}^{1/3} + A_{M_1}^{1/3}),\ r_c \approx 1.2 - 1.5\ \text{fm}]$. Therefore, the open reaction channels must meet the condition $E^* - E_{k_1} > B_1 + V_{\rm Coul}$. Obviously, the Coulomb barrier can effect the open reaction channels significantly. It is also obvious that $T_l(\varepsilon_{m_1}^c)$ is 0, if $\varepsilon_{m_1}^c \leqslant E_{\min}^{m_1}$.

Additionally, the total emission rate $W_T^{j\pi}(n,E^*)$ in pre-equilibrium reaction processes can be expressed as

$$W_T^{j\pi}(n,E^*) = \sum_{m_1,k_1} W_{m_1,k_1}^{j\pi}\left(n,E^*,\varepsilon_{m_1}^c\right). \tag{11}$$

In equilibrium reaction processes, the partial emission rate of the first particle m_1 in the $j\pi$ channel and the total emission rate can be derived as follows [36]:

$$W_{m_1,k_1}^{j\pi}\left(E^*,\varepsilon_{m_1}^c\right) = \frac{1}{2\pi\hbar\rho^{j\pi}(E^*)} \sum_{J=|j-I_{M_1}|}^{j+I_{M_1}} \sum_{l=|J-s_{m_1}|}^{J+s_{m_1}} \times (2J+1) T_{Jl}\left(\varepsilon_{m_1}^c\right) g_l\left(\pi,\pi_{k_1}\right), \tag{12}$$

$$W_T^{j\pi}(E^*) = \sum_{m_1,k_1} W_{m_1,k_1}^{j\pi}\left(E^*,\varepsilon_{m_1}^c\right), \tag{13}$$

where s_{m_1} and I_{M_1} are the spins of the emitted particle m_1 and the corresponding residual nucleus M_1, respectively. $T_{Jl}(\varepsilon_{m_1}^c)$ is the penetration factor, and $\rho^{j\pi}(E^*)$ is the energy level density.

2. *Secondary particle emission process*

After the first particle m_1 emission, the cross section of the first residual nucleus M_1 at energy level E_{k_1} emitting the secondary particle m_2 to the secondary residual nucleus M_2 at energy level E_{k_2} can be expressed in the frame of STLN as follows:

$$W_{m_2}^{j_{k_1}\pi_{k_1}\to j_{k_2}\pi_{k_2}}\left(E_{k_1} \to E_{k_2}\right) = \frac{1}{2\pi} \sum_{S=|j_{k_2}-s_{m_2}|}^{j_{k_2}+s_{m_2}} \sum_{l=|j_{k_1}-S|}^{j_{k_1}+S} T_l\left(\varepsilon_{m_2}^r\right) g_l\left(\pi_{k_1},\pi_{k_2}\right), \tag{14}$$

where $j_{k_1}\pi_{k_1}$ and $j_{k_2}\pi_{k_2}$ are the angular momenta and parities of the first and secondary residual nuclei, respectively. $T_l(\varepsilon_{m_2}^r)$ is the reduced penetration factor of the secondary emitted particle m_2, and $g_l(\pi_{k_1},\pi_{k_2})$ denotes the parity conservation in the secondary particle emission process.

The kinetic energy of the secondary emitted particle m_2 in the recoil nucleus system (RNS) is expressed as

$$\varepsilon_{m_2}^r = \frac{M_2}{M_1}\left(E_{k_1} - B_2 - E_{k_2}\right). \tag{15}$$

As well as m_1, there is a threshold energy $E_{\min}^{m_2}$ if the secondary emitted particle m_2 is a charged particle because of the Coulomb barrier.

The total emission rate $W_T^{j_{k_1}\pi_{k_1}}(E_{k_1})$ from the first residual nucleus at energy level E_{k_1} can be expressed as

$$W_T^{j_{k_1}\pi_{k_1}}\left(E_{k_1}\right) = W_\gamma^{j_{k_1}\pi_{k_1}}\left(E_{k_1}\right) + \sum_{m_2,k_2} W_{m_2}^{j_{k_1}\pi_{k_1}\to j_{k_2}\pi_{k_2}}\left(E_{k_1} \to E_{k_2}\right), \tag{16}$$

where $W_\gamma^{j_{k_1}\pi_{k_1}}(E_{k_1})$ is the deexcited rate of the γ photon from energy level E_{k_1}.

So the branching ratio of the secondary emitted particle m_2 from energy level E_{k_1} of M_1 to the energy level E_{k_2} of M_2 can be expressed as

$$R_{m_2}^{k_1\to k_2}\left(E_{k_1}\right) = \frac{W_{m_2}^{j_{k_1}\pi_{k_1}\to j_{k_2}\pi_{k_2}}\left(E_{k_1} \to E_{k_2}\right)}{W_T^{j_{k_1}\pi_{k_1}}\left(E_{k_1}\right)}. \tag{17}$$

Similarly, the branching ratio of γ photon can also be written as

$$R_\gamma^{k_1}\left(E_{k_1}\right) = \frac{W_\gamma^{j_{k_1}\pi_{k_1}}\left(E_{k_1}\right)}{W_T^{j_{k_1}\pi_{k_1}}\left(E_{k_1}\right)}. \tag{18}$$

Thus, the cross section of the secondary particle m_2 emitted from the energy level E_{k_1} of M_1 to E_{k_2} of M_2 can be expressed as

$$\sigma_{k_1\to k_2}(n,m_1,m_2) = \sigma_{k_1}(n,m_1) R_{m_2}^{k_1\to k_2}\left(E_{k_1}\right). \tag{19}$$

If the energy level E_{k_1} of M_1 is only deexcited by the γ photon to finish the reaction processes, the cross section of the first particle emission channel reads as

$$\sigma_{k_1}(n,m_1,\gamma) = \sigma_{k_1}(n,m_1) R_\gamma^{k_1}\left(E_{k_1}\right). \tag{20}$$

Equations (17)–(20) describe the competitions among the reaction channels of the first particle emission, secondary particle emission, and γ deexcitation. In addition, the (reduced) penetration factor T can be derived by the optical model to fit the cross sections of all of the channels.

B. Kinematics

1. *First particle emission process*

After the first particle m_1 is emitted, the residual nucleus M_1 may remain at the energy level E_{k_1}. Considering the energy-momentum conservation in CMS, the definitive kinetic energies of m_1 and M_1 can be reexpressed to systematically describe the kinematics as

$$\varepsilon_{m_1}^c = \frac{M_1}{M_C}\left(E^* - B_1 - E_{k_1}\right) \tag{21}$$

and

$$E_{M_1}^c = \frac{m_1}{M_C}\left(E^* - B_1 - E_{k_1}\right). \tag{22}$$

The normalized angular distributions of the first emitted particle m_1 and its residual nucleus M_1 with definitive kinetic energies can be standardized in nuclear reaction databases as [10]

$$\frac{d\sigma}{d\Omega_Y^c} = \sum_l \frac{2l+1}{4\pi} f_l^c(Y) P_l\left(\cos\theta_Y^c\right). \tag{23}$$

Here, $Y = m_1$ or M_1. $P_l(x)$ is the Legendre function, and the Legendre expansion coefficients $f_l^c(M_1) = (-1)^l f_l^c(m_1)$ can be derived from the the generalized master equation of the exciton model [38].

Using the nonrelativistic triangle relationship of the velocity vectors, the average kinetic energy of the first emitted particle m_1 in LS can be obtained:

$$\begin{aligned}\overline{\varepsilon}^l_{m_1} &= \int \frac{1}{2} m_1 \left(\boldsymbol{V}_C + \boldsymbol{v}^c_{m_1}\right)^2 \frac{d\sigma}{d\Omega^c_{m_1}} d\Omega^c_{m_1} \\ &= \frac{m_1 m_0 E_L}{M_C^2} + \varepsilon^c_{m_1} + \frac{2}{M_C}\sqrt{m_0 m_1 E_L \varepsilon^c_{m_1}}\, f_1^c(m_1), \quad (24)\end{aligned}$$

where $\boldsymbol{V}_C$ and $\boldsymbol{v}^c_{m_1}$ are the velocity vectors of the center of mass and the first emitted particle m_1 in CMS, respectively. Similarly to Eq. (24), the average kinetic energy of the first residual nucleus M_1 in LS reads

$$\overline{E}^l_{M_1} = \frac{M_1 m_0 E_L}{M_C^2} + E^c_{M_1} - \frac{2M_1}{M_C}\sqrt{\frac{m_0 E_L E^c_{M_1}}{M_1}}\, f_1^c(m_1). \quad (25)$$

Thus, it is obvious that the energy conservation for the first particle emission process in LS can be strictly kept as follows:

$$E^l_{\text{total}} = \overline{\varepsilon}^l_{m_1} + \overline{E}^l_{M_1} + E_{k_1} = E_L + B_0 - B_1. \quad (26)$$

2. *Secondary particle emission processes*

For the $1p$-shell light nucleus reactions, the secondary particle emission processes also come from the discrete energy levels after the first particle m_1 emission. There are four kinds the particle emission processes, as follows.

(1) The residual nucleus M_1 at energy level E_{k_1} emits the secondary particle m_2 with kinetic energy $\varepsilon^c_{m_2}$ to the secondary residual nucleus M_2 at energy level E_{k_2}.
(2) The residual nucleus M_1 at energy level E_{k_1} spontaneously breaks up into two particles.
(3) The first emitted particle m_1, such as ^{5}He, which is very unstable, spontaneously breaks up into a neutron and an α.
(4) All of the first emitted particles m_1 and their residual nuclei M_1 are unstable and spontaneously break up into two smaller particles or nuclei. This is the so-called double two-body breakup reaction.

For case (1), the residual nucleus M_1 at energy level E_{k_1} with recoiling kinetic energy $E^c_{M_1}$ in CMS will emit the secondary particle m_2 with kinetic energy $\varepsilon^c_{m_2}$, if the conservations of energy, angular momentum, and parity are met. Thus, the corresponding residual nucleus M_2 at energy level E_{k_2} will also gain the recoiling kinetic energy $E^c_{M_2}$ at arbitrary directions in CMS. In order to analytically describe the kinematics of the secondary emitted particle, we assume M_1 is static in RNS, then the definitive kinetic energy of the secondary emitted particle m_2 can be expressed as

$$\varepsilon^r_{m_2} = \frac{M_2}{M_1}\left(E_{k_1} - B_2 - E_{k_2}\right). \quad (27)$$

Similarly, the energy of the residual nucleus M_2 in the RNS can be also obtained

$$E^r_{M_2} = \frac{m_2}{M_1}\left(E_{k_1} - B_2 - E_{k_2}\right). \quad (28)$$

Using the nonrelativistic triangle relationship $\boldsymbol{v}^c_{m_2} = \boldsymbol{v}^c_{M_1} + \boldsymbol{v}^r_{m_2}$, we can obtain [29,30]

$$\varepsilon^c_{m_2} = \varepsilon^r_{m_2}(1 + 2\gamma\cos\Theta + \gamma^2), \quad (29)$$

$$\begin{aligned}\cos\Theta = \sqrt{\frac{\varepsilon^c_{m_2}}{\varepsilon^r_{m_2}}}\big[&\cos\theta^c_{m_2}\cos\theta^c_{M_1} \\ &+ \sin\theta^c_{m_2}\sin\theta^c_{M_1}\cos\left(\varphi^c_{m_2} - \varphi^c_{M_1}\right)\big] - \gamma, \quad (30)\end{aligned}$$

where $\gamma \equiv \sqrt{\frac{m_2 E^c_{M_1}}{M_1 \varepsilon^r_{m_2}}}$. The maximum and minimum kinetic energies of the secondary emitted particle m_2 in CMS are given by

$$\varepsilon^c_{m_2,\,\max} = \varepsilon^r_{m_2}(1+\gamma)^2, \quad \varepsilon^c_{m_2,\,\min} = \varepsilon^r_{m_2}(1-\gamma)^2. \quad (31)$$

In the frame of STLN, the double-differential cross section of the secondary emitted particle m_2 in RNS is assumed to have an isotropic distribution with a definitive kinetic energy $\varepsilon^r_{m_2}$, i.e.,

$$\frac{d^2\sigma}{d\varepsilon^r_{m_2} d\Omega^r_{m_2}} = \frac{1}{4\pi}\delta\left[\varepsilon^c_{m_2} - \varepsilon^r_{m_2}(1 + 2\gamma\cos\Theta + \gamma^2)\right]. \quad (32)$$

Starting from the basic relation of the double-differential cross sections between CMS and RNS, the double-differential cross section of m_2 in CMS can be obtained through the corresponding results in RNS averaged by the angular distribution of the residual nucleus M_1, i.e.,

$$\frac{d^2\sigma}{d\varepsilon^c_{m_2} d\Omega^c_{m_2}} = \int d\Omega^c_{M_1} \frac{d\sigma}{d\Omega^c_{M_1}} \sqrt{\frac{\varepsilon^c_{m_2}}{\varepsilon^r_{m_2}}} \frac{d^2\sigma}{d\varepsilon^r_{m_2} d\Omega^r_{m_2}}. \quad (33)$$

By means of the properties of the δ function and Eqs. (23)–(33), the double-differential cross section of the secondary emitted particle m_2 in CMS can be rewritten as [8,41]

$$\begin{aligned}&\frac{d^2\sigma}{d\varepsilon^c_{m_2} d\Omega^c_{m_2}} \\ &= \frac{1}{16\pi^2\gamma\varepsilon^r_{m_2}} \sum_l (2l+1) f_l^c(M_1) \\ &\quad \times \int_0^\pi dt\, P_l\left(\sqrt{(1-\eta^2)\sin^2\theta^c_{m_2}}\cos t + \eta\cos\theta^c_{m_2}\right), \quad (34)\end{aligned}$$

where $\eta = \sqrt{\frac{\varepsilon^r_{m_2}}{\varepsilon^c_{m_2}}}\frac{\varepsilon^c_{m_2}/\varepsilon^r_{m_2} - 1 + \gamma^2}{2\gamma}$. In terms of the new integral formula [41], which has not been compiled in any integral tables or mathematical software, Eq. (34) can be simplified as

$$\frac{d^2\sigma}{d\varepsilon^c_{m_2} d\Omega^c_{m_2}} = \sum_l \frac{(-1)^l}{16\pi\gamma\varepsilon^r_{m_2}} (2l+1) f_l^c(m_1) P_l(\eta) P_l\left(\cos\theta^c_{m_2}\right). \quad (35)$$

The normalized double-differential cross section of the secondary emitted particle m_2 is also standardized in nuclear reaction databases as [10]

$$\frac{d^2\sigma}{d\varepsilon^c_{m_2}d\Omega^c_{m_2}} = \sum_l \frac{2l+1}{4\pi} f^c_l(m_2)P_l\left(\cos\theta^c_{m_2}\right). \quad (36)$$

By comparing Eqs. (35) and (36), the Legendre expansion coefficients of the secondary emitted particle m_2 in CMS can be expressed as

$$f^c_l(m_2) = \frac{(-1)^l}{4\gamma\varepsilon^r_{m_2}} f^c_l(m_1)P_l(\eta). \quad (37)$$

Similarly to Eq. (37), we can also derive the analytical expression of the Legendre expansion coefficients of the secondary residual nucleus M_2 in CMS. The formula is expressed as [41]

$$f^c_l(M_2) = \frac{(-1)^l}{4\Gamma E^r_{M_2}} f^c_l(m_1)P_l(H), \quad (38)$$

where $\Gamma = \sqrt{\frac{M_2E^c_{M_1}}{M_1E^r_{M_2}}}$ and $H = \sqrt{\frac{E^r_{M_2}}{E^c_{M_2}}}\frac{E^c_{M_2}/E^r_{M_2}-1+\Gamma^2}{2\Gamma}$.

It is obvious that the Legendre expansion coefficients of the secondary emitted particle m_2 and its residual nucleus M_2 in CMS are closely related to the first emitted particle m_1 and its recoiling nucleus M_1. Analytical expressions of Eq. (37) and (38) can largely reduce the volume of file-6 in nuclear reaction databases.

In CMS, the average kinetic energy of the secondary emitted particle m_2 can be obtained by averaging its double differential cross section, i.e.,

$$\begin{aligned}\overline{\varepsilon}^c_{m_2} &= \int_{\varepsilon^c_{m_2,\min}}^{\varepsilon^c_{m_2,\max}} \varepsilon^c_{m_2}\frac{d^2\sigma}{d\varepsilon^c_{m_2}d\Omega^c_{m_2}}d\varepsilon^c_{m_2}d\Omega^c_{m_2} \\ &= \varepsilon^r_{m_2}(1+\gamma^2). \end{aligned} \quad (39)$$

We also can obtain the average kinetic energy of the secondary residual nucleus M_2 in CMS in the same way, i.e.,

$$\overline{\varepsilon}^c_{M_2} = E^r_{M_2}(1+\Gamma^2). \quad (40)$$

In terms of the nonrelativistic triangle relationship of the velocity vectors, the average kinetic energy of the secondary emitted particle m_2 in LS can be obtained

$$\begin{aligned}\overline{\varepsilon}^l_{m_2} &= \int \frac{1}{2}m_2\left(\boldsymbol{V}_C + \boldsymbol{v}^c_{m_2}\right)^2\frac{d^2\sigma}{d\varepsilon^c_{m_2}d\Omega^c_{m_2}}d\varepsilon^c_{m_2}d\Omega^c_{m_2} \\ &= \frac{m_0m_2E_L}{M_C^2} + \overline{\varepsilon}^c_{m_2} - 2\frac{m_2}{M_C}\sqrt{\frac{m_0E_LE^c_{M_1}}{M_1}}f^c_1(m_1). \end{aligned} \quad (41)$$

In the same way, the average kinetic energy of the secondary residual nucleus M_2 in LS can be derived as

$$\overline{E}^l_{M_2} = \frac{m_0M_2E_L}{M_C^2} + \overline{E}^c_{M_2} - 2\frac{M_2}{M_C}\sqrt{\frac{m_0E_LE^c_{M_1}}{M_1}}f^c_1(m_1). \quad (42)$$

Thus, the energy conservation of the initial and final states for the light nucleus reactions can be strictly kept in LS as follows:

$$\begin{aligned}E^l_{\text{total}} &= \overline{\varepsilon}^l_{m_1} + \overline{\varepsilon}^l_{m_2} + \overline{E}^l_{M_2} + E_{k_2} \\ &= E_L + B_0 - B_1 - B_2. \end{aligned} \quad (43)$$

For case (2), the residual nucleus M_1 at energy level E_{k_1} spontaneously break up into two smaller particles m_2 and M_2. It is assumed that m_2 and M_2 are at ground states, i.e., $E_{k_2} = 0$. As in case (1), we assume M_1 is static in RNS, then the definitive kinetic energies of m_2 and M_2 can be expressed as

$$\varepsilon^r_{m_2} = \frac{M_2}{M_1}\left(E_{k_1} + Q_{M_2}\right) \quad (44)$$

and

$$E^r_{M_2} = \frac{m_2}{M_1}\left(E_{k_1} + Q_{M_2}\right), \quad (45)$$

where Q_{M_2} is the reaction Q value for the breakup process $M_1 \to m_2 + M_2$.

Similarly, we can obtain the average kinetic energies of m_2 and M_2 in CMS as follows:

$$\overline{\varepsilon}^c_{m_2} = \frac{M_2}{M_1}\left(E_{k_1} + Q_{M_2}\right) + \frac{m_1m_2}{M_1^2}\varepsilon^c_{m_1} \quad (46)$$

and

$$\overline{E}^c_{M_2} = \frac{m_2}{M_1}\left(E_{k_1} + Q_{M_2}\right) + \frac{m_1M_2}{M_1^2}\varepsilon^c_{m_1}. \quad (47)$$

Furthermore, we can obtain the average kinetic energies of m_2 and M_2 in LS as follows:

$$\overline{\varepsilon}^l_{m_2} = \frac{m_0m_2E_L}{M_C^2} + \overline{\varepsilon}^c_{m_2} - \frac{2m_2}{M_CM_1}\sqrt{m_0m_1E_L\varepsilon^c_{m_1}}f^c_1(m_1) \quad (48)$$

and

$$\overline{E}^l_{M_2} = \frac{m_0M_2E_L}{M_C^2} + \overline{E}^c_{M_2} - \frac{2M_2}{M_CM_1}\sqrt{m_0m_1E_L\varepsilon^c_{m_1}}f^c_1(m_1) \quad (49)$$

Obviously, the energy conservation of the initial and final states can be strictly kept in LS as follows:

$$\begin{aligned}E^l_{\text{total}} &= \overline{\varepsilon}^l_{m_1} + \overline{\varepsilon}^l_{m_2} + \overline{E}^l_{M_2} \\ &= E_L + B_0 - B_1 + Q_{M_2}. \end{aligned} \quad (50)$$

For case (3), the first emitted particle m_1 can spontaneously break up into two smaller particles. For the $1p$-shell light nucleus reactions, the unstable nucleus m_1 is only ^{5}He, which spontaneously breaks up into a neutron (m_n) and an α (M_α). As in case (1), we assume that m_1 is static in RNS. Then the definitive kinetic energies of m_n and M_α can be expressed as

$$\varepsilon^r_n = \frac{M_\alpha}{m_1}Q_{m_1} \quad (51)$$

and

$$E^r_\alpha = \frac{m_n}{m_1}Q_{m_1}, \quad (52)$$

where Q_{m_1} is the reaction Q value for the breakup process $^5\text{He} \to n + \alpha$.

Similarly, we can obtain the average kinetic energies of m_n and M_α in CMS as follows:

$$\overline{\varepsilon}^c_{m_n} = \frac{M_\alpha}{m_1} Q_{m_1} + \frac{m_n}{m_1}\varepsilon^c_{m_1} \tag{53}$$

and

$$\overline{E}^c_{M_\alpha} = \frac{m_n}{m_1} Q_{m_1} + \frac{M_\alpha}{m_1}\varepsilon^c_{m_1}. \tag{54}$$

Furthermore, we can obtain the average kinetic energies of m_n and M_α in LS as follows:

$$\overline{\varepsilon}^l_{m_n} = \frac{m_0 m_n E_L}{M_C^2} + \overline{\varepsilon}^c_{m_n} + \frac{2m_n}{M_C m_1}\sqrt{m_0 m_1 E_L \varepsilon^c_{m_1}}\, f_1^c(m_1) \tag{55}$$

and

$$\overline{E}^l_{M_\alpha} = \frac{m_0 M_\alpha E_L}{M_C^2} + \overline{E}^c_{M_\alpha} + \frac{2M_\alpha}{M_C m_1}\sqrt{m_0 m_1 E_L \varepsilon^c_{m_1}}\, f_1^c(m_1). \tag{56}$$

Obviously, the energy conservation of the initial and final states can be strictly kept in LS as follows:

$$\begin{aligned} E^l_{\text{total}} &= \overline{E}^l_{M_1} + \overline{\varepsilon}^l_{m_n} + \overline{E}^l_{M_\alpha} \\ &= E_L + B_0 - B_1 + Q_{m_1}. \end{aligned} \tag{57}$$

It is worth mentioning that the symbols before the Legendre expansion coefficients $f_1^c(m_1)$ of m_n and M_α are positive in case (3), compared to the negative signs in other cases. This is due to the forward tendency of the first emitted particle m_1.

For case (4), all of the first emitted particles m_1 and their residual nuclei M_1 can spontaneously break up into two smaller particles at the same time. As in case (2), the averaged kinetic energies of m_2 and M_2 in both CMS and LS coming from the residual nucleus M_1 can be expressed as Eqs. (44)–(49). For this double two-body breakup process of the $1p$-shell light nucleus reactions, the first emitted particle m_1 is ^{5}He, which can spontaneously break up into a neutron (m_n) and an α (M_α). The averaged kinetic energies of the neutron (m_n) and α (M_α) in both CMS and LS coming from ^{5}He can be expressed as Eqs. (51)–(56). Thus, the energy conservation of the initial and final states can be strictly kept in LS as follows:

$$\begin{aligned} E^l_{\text{total}} &= \overline{E}^l_{M_2} + \overline{\varepsilon}^l_{m_2} + \overline{E}^l_{M_\alpha} + \overline{\varepsilon}^l_{m_n} \\ &= E_L + B_0 - B_1 + Q_{m_1} + Q_{M_2}. \end{aligned} \tag{58}$$

III. APPLICATIONS TO $p + {}^9$Be REACTIONS

For neutron induced nuclear reactions with $1p$-shell light nuclei involved, such as ^{6}Li [24], ^{7}Li [25], ^{9}Be [26,27], ^{10}B [28], ^{11}B [29], ^{12}C [7,30,31], ^{14}N [32], ^{16}O [33,34], and ^{19}F [35], the calculated double-differential cross sections of outgoing neutrons agree very well with the experimental data. In this section, taking $p + {}^9$Be reaction at 18 MeV as an example, we analyze the open reaction channels in detail at 18 MeV, and calculate the double-differential cross sections of outgoing neutrons using the PUNF code in the frame of STLN. The calculated results are compared with the existing experimental data, and the partial double-differential cross sections of outgoing neutron from possible energy levels are shown in detail.

A. Analysis of the reaction channels

For the proton induced ^{9}Be reaction, theoretically reaction channels exist at incident energy $E_p \leqslant 20$ MeV in terms of the reaction threshold energies E_{th} as follows:

$$p + {}^9\text{Be} \rightarrow {}^{10}\text{B}^* \rightarrow \begin{cases} (p,\gamma)\,{}^{10}\text{B}, & Q = +6.586\ \text{MeV}, & E_{th} = 0.000\ \text{MeV}, \\ (p,n)\,{}^{9}\text{B}, & Q = -1.850\ \text{MeV}, & E_{th} = 2.067\ \text{MeV}, \\ (p,p)\,{}^{9}\text{Be}, & Q = 0.000\ \text{MeV}, & E_{th} = 0.000\ \text{MeV}, \\ (p,\alpha)\,{}^{6}\text{Li}, & Q = +2.127\ \text{MeV}, & E_{th} = 0.000\ \text{MeV}, \\ (p,{}^3\text{He})\,{}^{7}\text{Li}, & Q = -11.202\ \text{MeV}, & E_{th} = 12.455\ \text{MeV}, \\ (p,d)\,{}^{8}\text{Be}, & Q = +0.559\ \text{MeV}, & E_{th} = 0.000\ \text{MeV}, \\ (p,{}^5\text{He})\,{}^{5}\text{Li}, & Q = -4.434\ \text{MeV}, & E_{th} = 4.930\ \text{MeV}, \\ (p,np)\,{}^{8}\text{Be}, & Q = -1.665\ \text{MeV}, & E_{th} = 1.851\ \text{MeV}, \\ (p,n\alpha)\,{}^{5}\text{Li}, & Q = -3.539\ \text{MeV}, & E_{th} = 3.935\ \text{MeV}, \\ (p,pn)\,{}^{8}\text{Be}, & Q = -1.665\ \text{MeV}, & E_{th} = 1.851\ \text{MeV}, \\ (p,p\alpha)\,{}^{5}\text{He}, & Q = -2.467\ \text{MeV}, & E_{th} = 2.743\ \text{MeV}, \\ (p,\alpha n)\,{}^{5}\text{Li}, & Q = -3.539\ \text{MeV}, & E_{th} = 3.935\ \text{MeV}, \\ (p,\alpha p)\,{}^{5}\text{He}, & Q = -2.467\ \text{MeV}, & E_{th} = 2.743\ \text{MeV}. \end{cases} \tag{59}$$

Considering the conservations of the energy, angular momentum, and parity in the particle emission processes, the reaction channels of the first particle emission are listed as follows:

$$p + {}^{9}\mathrm{Be} \rightarrow {}^{10}\mathrm{B}^{*} \rightarrow \begin{cases} n + {}^{9}\mathrm{B}^{*}\ (k_1 = \mathrm{gs},1,2,\ldots,10), \\ p + {}^{9}\mathrm{Be}^{*}\ (k_1 = \mathrm{gs},1,2,\ldots,21), \\ \alpha + {}^{6}\mathrm{Li}^{*}\ (k_1 = \mathrm{gs},1,2,\ldots,7), \\ {}^{3}\mathrm{He} + {}^{7}\mathrm{Li}^{*}\ (k_1 = \mathrm{gs},1,2,\ldots,4), \\ d + {}^{8}\mathrm{Be}^{*}\ (k_1 = \mathrm{gs},1,2,\ldots,8), \\ t + {}^{7}\mathrm{Be}\ (k_1 = \mathrm{gs}), \\ {}^{5}\mathrm{He} + {}^{5}\mathrm{Li}^{*}\ (k_1 = \mathrm{gs},1), \end{cases} \tag{60}$$

where gs and k_1 denote the ground state and the k_1th energy level of the residual nuclei M_1, respectively.

For the first particle emission channel ${}^{9}\mathrm{Be}(p,n){}^{9}\mathrm{B}^{*}$, the first residual nucleus ${}^{9}\mathrm{B}^{*}$ can still emit a proton at some excited energy levels, and the secondary residual nucleus ${}^{8}\mathrm{Be}^{*}$ can spontaneously break up into two α [28]. Thus, these reaction processes belong to the reaction channel ${}^{9}\mathrm{Be}(p,np2\alpha)$ at the final state.

For reaction channel ${}^{9}\mathrm{Be}(p,p){}^{9}\mathrm{Be}^{*}$, if the first residual nucleus ${}^{9}\mathrm{Be}^{*}$ is at ground state, then this channel belongs to the compound nucleus elastic scattering. If the first residual nucleus ${}^{9}\mathrm{Be}^{*}$ is at the k_1th ($k_1 \geqslant 1$) excited energy level, some energy levels will emit a neutron and the secondary residual nucleus ${}^{8}\mathrm{Be}^{*}$ can spontaneously break up into two α. Thus, these reaction processes also belong to the reaction channel ${}^{9}\mathrm{Be}(p,np2\alpha)$ at the final state. Especially, if the first residual nucleus ${}^{9}\mathrm{Be}^{*}$ is at the k_1th ($k_1 \geqslant 4$) excited energy level, some energy levels may emit an α, and the secondary residual nucleus ${}^{5}\mathrm{He}^{*}$ can also spontaneously break up into a neutron and an α. Thus, this reaction process also belongs to the reaction channel ${}^{9}\mathrm{Be}(p,np2\alpha)$ at the final state. Therefore, the particle emission processes of the first residual nucleus ${}^{9}\mathrm{Be}^{*}$ can be described as follows [26,27]:

$${}^{9}\mathrm{Be}^{*} \rightarrow \begin{cases} k = \mathrm{gs}, & (p,p){}^{9}\mathrm{Be}, \\ k \geqslant 1,\ n + {}^{8}\mathrm{Be}^{*} \rightarrow 2\alpha, & (p,np2\alpha), \\ k \geqslant 4,\ \alpha + {}^{5}\mathrm{He}^{*} \rightarrow n + \alpha, & (p,np2\alpha). \end{cases} \tag{61}$$

For reaction channel ${}^{9}\mathrm{Be}(p,\alpha){}^{6}\mathrm{Li}^{*}$, the first residual nucleus ${}^{6}\mathrm{Li}^{*}$ may emit a neutron at different excited energy levels through ${}^{6}\mathrm{Li}^{*} \rightarrow p + {}^{5}\mathrm{He}$ (${}^{5}\mathrm{He} \rightarrow n + \alpha$) and ${}^{6}\mathrm{Li}^{*} \rightarrow n + {}^{5}\mathrm{Li}$ (${}^{5}\mathrm{Li} \rightarrow p + \alpha$) [24,25], but the cross section of this first particle emission process is so small that its contribution to neutron products can be reasonably neglected.

For reaction channel ${}^{9}\mathrm{Be}(p,{}^{3}\mathrm{He}){}^{7}\mathrm{Li}^{*}$ at $E_p = 18$ MeV, the first residual nucleus ${}^{7}\mathrm{Li}^{*}$ [24,25] only at the ground, first, and second excited energy levels cannot emit neutron. So the contributions of this reaction channel to neutron products are not considered in this work, as well as the reaction channels ${}^{9}\mathrm{Be}(p,d){}^{8}\mathrm{Be}^{*}$ and ${}^{9}\mathrm{Be}(p,t){}^{7}\mathrm{Be}^{*}$.

In addition, the double two-body breakup reaction ${}^{9}\mathrm{B}^{*}(p,{}^{5}\mathrm{He}^{*}){}^{5}\mathrm{Li}^{*}$ also belongs to channel $(p,np2\alpha)$ through breakup reactions ${}^{5}\mathrm{He} \rightarrow n + \alpha$ and ${}^{5}\mathrm{Li} \rightarrow p + \alpha$. In conclusion, for the proton induced ${}^{9}\mathrm{Be}$ reaction, reaction channels exist at incident energy $E_p \leqslant 20$ MeV as follows:

$$p + {}^{9}\mathrm{Be} \rightarrow {}^{10}\mathrm{B}^{*} \rightarrow \begin{cases} n + {}^{9}\mathrm{B}^{*} & (k_1 = \mathrm{gs},1,\ldots,10) \rightarrow p + {}^{8}\mathrm{Be}^{*} \rightarrow 2\alpha, & (p,np2\alpha), \\ p + {}^{9}\mathrm{Be}^{*} & (k_1 = \mathrm{gs}), \quad \text{compound nucleus elastic} & \text{scattering} \\ & (k_1 \geqslant 1) \rightarrow n + {}^{8}\mathrm{Be}^{*} \rightarrow 2\alpha, & (p,np2\alpha), \\ & (k_1 \geqslant 4) \rightarrow \alpha + {}^{5}\mathrm{He}^{*} \rightarrow n + \alpha, & (p,np2\alpha), \\ \alpha + {}^{6}\mathrm{Li}^{*} & (k_1 = \mathrm{gs},2), & (p,\alpha){}^{6}\mathrm{Li}, \\ & (k_1 = 1,3,4,\ldots,7) \rightarrow d + \alpha, & (p,d2\alpha), \\ {}^{3}\mathrm{He} + {}^{7}\mathrm{Li}^{*} & (k_1 = \mathrm{gs},1,2,3), & (p,{}^{3}\mathrm{He}){}^{7}\mathrm{Li}, \\ d + {}^{8}\mathrm{Be}^{*} & (k_1 = \mathrm{gs},1,\ldots,8) \rightarrow 2\alpha, & (p,d2\alpha), \\ t + {}^{7}\mathrm{Be} & (k_1 = \mathrm{gs}), & (p,t){}^{7}\mathrm{Be}, \\ {}^{5}\mathrm{He} + {}^{5}\mathrm{Li}^{*} & (k_1 = \mathrm{gs},1) \rightarrow n + \alpha + p + \alpha, & (p,np2\alpha). \end{cases} \tag{62}$$

From Eq. (62), one can see that the contributions to the double-differential cross sections of outgoing neutrons only come from reaction channel $(p,np2\alpha)$, which consists of four kinds of particle emission processes.

B. Calculation of the double-differential cross sections of outgoing neutrons

In the case of the $p + {}^{9}\mathrm{Be}$ reaction at $E_p = 18$ MeV with outgoing angle 60° in LS, the partial double-differential cross sections of outgoing neutrons from reaction channel $(p,n){}^{9}\mathrm{B}$ are shown in Fig. 1. The black lines denote the partial neutron spectra coming from the ground state to ninth excited energy levels ($k_1 = \mathrm{gs},1,\ldots,9$, as labeled in the figure) of the first residual nucleus ${}^{9}\mathrm{B}$. Because of the level widths and energy resolution in the measurements, the measured data are always in broadening form. Therefore, the broadening effect must be taken into account in the first particle emission processes [30]. Only the cross sections with values larger than 0.1 mb are given; this applies also to the following figures.

The partial double-differential cross sections of outgoing neutrons from reaction channel $(p,pn){}^{8}\mathrm{Be} \rightarrow (p,pn + 2\alpha)$

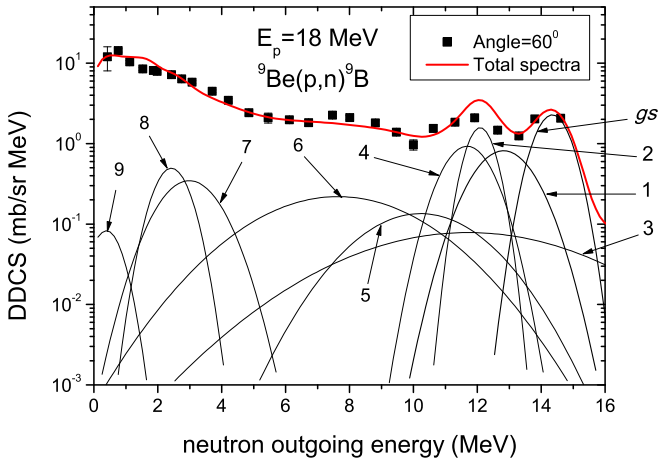

FIG. 1. The partial double-differential cross sections of outgoing neutrons from reaction channel $(p,n)^9$B with outgoing angle 60° at $E_p = 18$ MeV in LS. The points denote the experimental data taken from Ref. [42], and the red solid line denotes the calculated total double-differential cross sections. The black solid lines denote the partial spectra of the first emitted neutron from the compound nucleus to the ground state, up to the ninth excited energy levels (as labeled in the figure) of the first residual nucleus ^{9}B, in which broadening effects must be taken into account. Only the cross sections with values larger than 0.1 mb are given.

are shown in Fig. 2, but the black lines denote the partial spectra of the secondary emitted neutron from the k_1th excited energy levels ($k_1 = 1,2,\ldots,17$, as labeled in the figure) of the first residual nucleus ^{9}Be to the ground state of the secondary residual nucleus ^{8}Be. In Fig. 3, the black solid lines denote the partial spectra of the secondary emitted neutron from the k_1th excited energy levels ($k_1 = 6,\ldots,17$, as labeled in the figure) of the first residual nucleus ^{9}Be to the first excited energy level

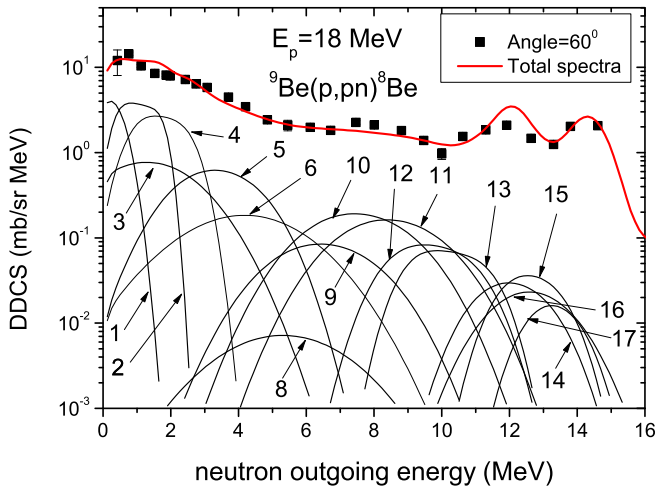

FIG. 2. The same as Fig. 1, but for the partial double-differential cross sections from reaction channel $(p,pn)^8\text{Be} \rightarrow (p,pn+2\alpha)$. The black solid lines denote the partial spectra of the secondary emitted neutron from the first to 17th excited energy levels (as labeled in the figure) of the first residual nucleus ^{9}Be to the ground state of the secondary residual nucleus ^{8}Be.

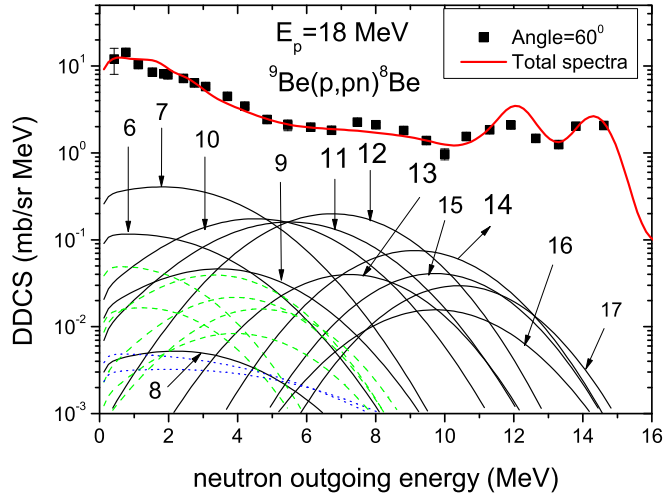

FIG. 3. The same as Fig. 2, but the black solid lines denote the partial spectra from the sixth to 17th excited energy levels (as labeled in the figure) of ^{9}Be to the first excited energy level of ^{8}Be. The green dashed lines denote the partial spectra from the 12th to 17th excited energy levels of ^{9}Be to the second excited energy level of ^{8}Be, and the blue dotted lines denote the partial spectra from the 14th and 17th excited energy levels of ^{9}Be to the third excited energy level of ^{8}Be.

of the secondary residual nucleus ^{8}Be. The green dashed lines denote the partial spectra of the secondary emitted neutron from the k_1th ($k_1 = 12,\ldots,17$) excited energy levels of the first residual nucleus ^{9}Be to the second excited energy level of the secondary residual nucleus ^{8}Be. The blue dotted lines denote the partial spectra of the secondary emitted neutron from the k_1th ($k_1 = 14,\ldots,17$) excited energy levels of the first residual nucleus ^{9}Be to the third excited energy level of the secondary residual nucleus ^{8}Be. But the calculated results show that the contributions (>0.1 mb) only come from two energy levels ($k_1 = 14$ and 17) of ^{9}Be.

In Fig. 4, the black solid lines denote the partial spectra of the emitted neutron from reaction channel $(p,p\alpha)^5\text{He} \rightarrow (p,p\alpha+n\alpha)$. The contributions of these partial neutron spectra come from the emissions between the fouth and 17th excited energy levels of the first residual nucleus ^{9}Be and the lowest two energy levels of the secondary residual nucleus ^{5}He, which can spontaneously break up into a neutron and an α. The blue dashed lines denote the partial spectra of the emitted neutron from reaction channel $(p,{}^5\text{He})^5\text{Li} \rightarrow (p,n\alpha+p\alpha)$. The contributions of these partial neutron spectra come from the ground state and the first excited energy level of ^{5}He.

Summing up all of the partial double-differential cross sections of outgoing neutrons, we can obtain the total double-differential cross sections at $E_p = 18$ MeV with outgoing angle 60° (as shown the red lines in Figs. 1–4). In these figures, the points denote the experimental data measured by Verbinski *et al.* [42]. One can see that the calculated total double-differential cross sections of outgoing neutrons agree very well with the experimental data. Similarly, the calculated total double-differential cross sections of outgoing neutrons at other angles also agree well with the experimental data as shown in Figs. 5 and 6. In addition, the calculated results are

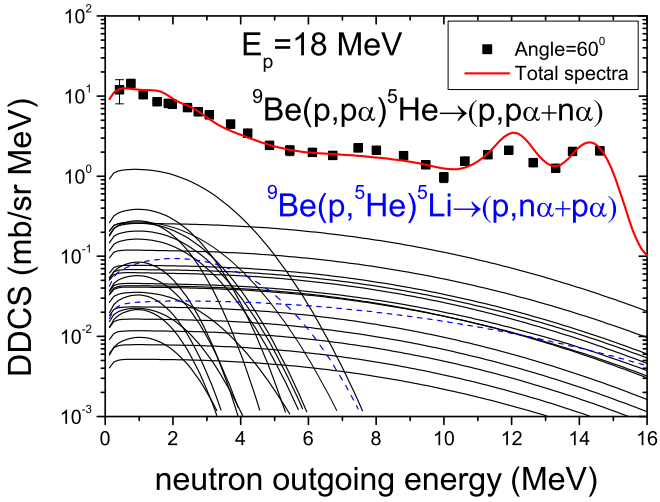

FIG. 4. The same as Fig. 1, but the black solid lines denote the partial spectra of the emitted neutron in reaction channel $(p,p\alpha)^5\mathrm{He} \rightarrow (p,p\alpha + n\alpha)$ from the fourth to 17th excited energy levels of ^{9}Be to the lowest two energy levels of the secondary residual nucleus ^{5}He, which can spontaneously break up a neutron and an α. The blue dashed lines denote the partial spectra of the emitted neutron in double two-body breakup channel $(p,{}^5\mathrm{He})^5\mathrm{Li} \rightarrow (p,n\alpha + p\alpha)$ from the ground state and first excited energy level of the ^{5}He.

slightly larger than the measured data in low outgoing neutron energy regions at angles 0° and 20°, as shown in Fig. 5. The reason is that the 4-mm-thick polyethylene beam stopper in the secondary Faraday cup slightly depresses the yields about 0.5–1.5 MeV at forward angles, as mentioned in Ref. [42].

We would like to state that all of the final states are the discrete levels of the residual nuclei in light nucleus reactions.

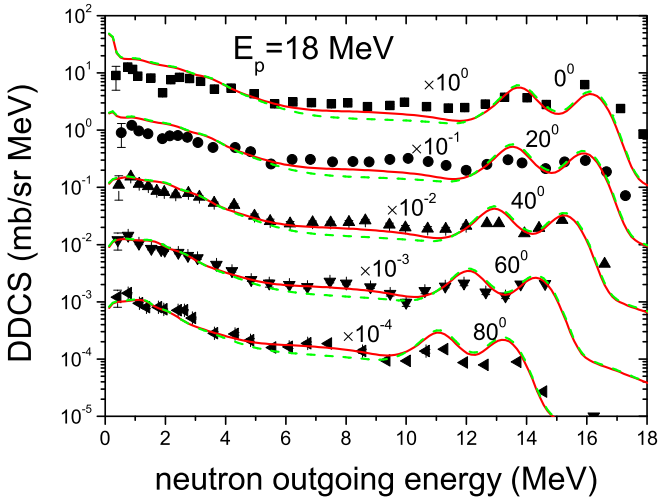

FIG. 5. The total double-differential cross sections of outgoing neutron for the reaction ^{9}Be(p,xn) with outgoing angles 0°, 20°, 40°, 60°, and 80° at $E_p = 18$ MeV in LS. The points denote to the experimental data taken from Ref. [42]. The red solid lines denote the calculated results using the real and two predicted energy levels of ^{9}Be, and the green dashed lines denote the calculated results only using the real energy levels of ^{9}Be.

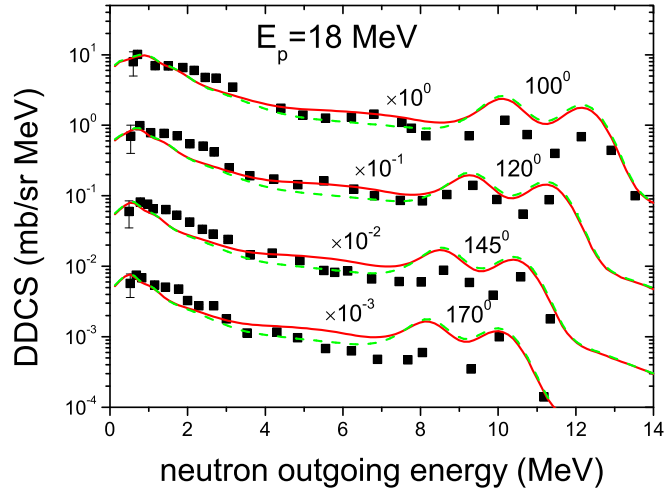

FIG. 6. The same as Fig. 5, but with outgoing angles 100°, 120°, 145°, and 170°, respectively.

Therefore, the theoretical calculations are very sensitive to the level schemes of the target and residual nuclei. Although the updated energy level schemes of the target and the residual nuclei [43,44] are employed for the reaction ^{9}Be(p,xn), the contributions coming from the real ninth and tenth energy levels of the target nucleus ^{9}Be, as shown by the green dashed lines in Figs. 5 and 6, are still deficient. So two predicted levels $9.0(\frac{5}{2}^+)$ and $10.0(\frac{5}{2}^+)$ between the ninth and tenth levels have been artificially added in this paper as neutron induced ^{9}Be reactions [26]. In Figs. 5 and 6, the red solid lines denote the results using the real energy levels and two predicted energy levels of ^{9}Be, and the green dashed lines denote the results only using the real energy levels. One can see that the calculated results of adding two predicted levels are in better agreement with the existing experimental data.

IV. SUMMARY

Our previous studies indicate that the calculated double-differential cross sections agree very well with the experimental data for neutron induced nuclear reactions with $1p$-shell light nuclei involved, which have been successfully used to set up file-6 in the CENDL 3.1 library. In this paper, STLN is proposed to describe the light particle (including neutron and light charged particles) induced nuclear reactions with $1p$-shell light nuclei involved. In the dynamics of STLN, not only the angular momentum and parity conservations for both equilibrium and pre-equilibrium processes but also the Coulomb barriers of the incoming and outgoing charged particles are considered in different particle emission processes. In the kinematics of STLN, the recoiling effects in various emission processes are strictly taken into account. Taking the ^{9}Be(p,xn) reaction as an example, we further calculate the double-differential cross sections of outgoing neutrons and charged particles using the PUNF code in the frame of STLN. The calculated results agree very well with the existing experimental neutron double-differential cross sections at $E_p = 18$ MeV, and indicate that the PUNF code

is a powerful tool to set up file-6 in the reaction data library for the light particle induced nuclear reactions with 1 p-shell light nuclei involved. However, one should note that STLN and the PUNF code are applied to nuclear reactions without polarization of incoming light particles and orientation of target nuclei.

In addition, two predicted levels of target nucleus ^{9}Be have been employed in this paper. The agreement between the calculated results and the experimental data shows again that there may be a lack of several levels of ^{9}Be. We hope these predicted levels could be validated by experiment in the future. For analytically describing the double-differential cross sections of reaction products in the sequential particle emission processes, a new integral formula, which has not been compiled in any integral tables or mathematical softwares, is employed to obtain analytical Legendre expansion coefficients. This integral formula can largely reduce the volume of file-6 in nuclear reaction databases with full energy balance. This integral formula and STLN are being tested by light charged particles induced nuclear reactions with 1 p-shell light nuclei involved.

ACKNOWLEDGMENTS

We thank Yun Guo, Shangui Zhou, Ning Wang, Li Ou, and Min Liu for some valuable suggestions. This work is supported by the National Natural Science Foundation of China (No. 11465005); the Natural Science Foundation of Guangxi (No. 2014GXNSFDA118003); Guangxi University Science and Technology Research Project (No. 2013ZD007); the Open Project Program of State Key Laboratory of Theoretical Physics, Institute of Theoretical Physics, Chinese Academy of Sciences, China (No. Y4KF041CJ1); and the project of outstanding young teachers' training in higher education institutions of Guangxi.

[1] P. Garin and M. Sugimoto, J. Nucl. Mater. **417**, 1262 (2011).
[2] J. Marder, B. Rath, and S. Obenschain, Adv. Mater. Process. **166**, 39 (2008).
[3] H. Kawamura, H. Takahashi, and N. Yoshida, Fusion Eng. Des. **61-62**, 391 (2002).
[4] C. G. Yu *et al.*, Ann. Nucl. Energy **85**, 597 (2015).
[5] Y. Mori, Nucl. Instrum. Methods A **562**, 591 (2006).
[6] W. L. Zhan, Accelerator driven advanced nuclear system & frontier researches, Report of the Institute of Theoretical Physics, Chinese Academy of Sciences, Beijing, 2015 (unpublished).
[7] X. J. Sun, W. J. Qu, J. F. Duan, and J. S. Zhang, Phys. Rev. C **78**, 054610 (2008).
[8] J. S. Zhang, *Statistical Theory of Neutron Induced Reactions of Light Nuclei*, 2nd ed. (in Chinese) (Science Press, Beijing, 2015).
[9] J. S. Zhang, Y. L. Han, and J. F. Duan, J. Korean Phys. Soc. **59**, 843 (2011).
[10] A. Trkov, M. Herman, and D. A. Brown, ENDF-6 Formats Manual, Brookhaven National Laboratory, Upton, NY, 2011.
[11] M. B. Chadwick, M. Herman, and P. Oblozinsky, Nucl. Data Sheets **112**, 2887 (2011).
[12] A. J. Koning and D. Rochman, Nucl. Data Sheets **113**, 2841 (2012).
[13] P. G. Young *et al.*, Transport Data Libraries for Incident Proton and Neutron Energies to 100 MeV, Los Alamos National Laboratory Report No. LA-11753-MS, 1990 (unpublished).
[14] A. J. Koning, S. Hilaire, and M. C. Duijvestijn, TALYS-1.0, *Proceedings of the International Conference on Nuclear Data for Science and Technology, Nice, France, 2007* (unpublished).
[15] Y. Iwamoto *et al.*, Nucl. Instrum. Methods A **598**, 687 (2009).
[16] S. Hashimoto *et al.*, Nucl. Data Sheets **118**, 258 (2014).
[17] H. Guo, Y. Watanabe, T. Matsumoto, K. Ogata, and M. Yahiro, Phys. Rev. C **87**, 024610 (2013).
[18] H. R. Guo, K. Nagaoka, Y. Watanabe, T. Matsumoto, K. Ogata, and M. Yahiro, Nucl. Data Sheets **118**, 254 (2014).
[19] T. Matsumoto, D. Ichinkhorloo, Y. Hirabayashi, K. Katō, and S. Chiba, Phys. Rev. C **83**, 064611 (2011).
[20] D. Ichinkhorloo, Y. Hirabayashi, K. Katō, M. Aikawa, T. Matsumoto, and S. Chiba, Phys. Rev. C **86**, 064604 (2012).
[21] J. S. Zhang, in *Proceedings of the Beijing International Symposium on Fast Neutron Physics, Beijing, September 1991*, edited by Z. Sun, H. Tang, J. Xu, and J. Zhang (World Scientific, Singapore, 1992), p. 193.
[22] J. S. Zhang, Nucl. Sci. Eng. **114**, 55 (1993).
[23] J. S. Zhang and Y. Q. Wen, Chin. J. Nucl. Phys. **16**, 153 (1994).
[24] J. S. Zhang, Commun. Theor. Phys. **36**, 437 (2001).
[25] J. S. Zhang and Y. L. Han, Commun. Theor. Phys. **37**, 465 (2002).
[26] J. F. Duan, J. S. Zhang, H. C. Wu, and X. J. Sun, Phys. Rev. C **80**, 064612 (2009).
[27] J. F. Duan, J. S. Zhang, H. C. Wu, and X. J. Sun, Commun. Theor. Phys. **54**, 129 (2010).
[28] J. S. Zhang, Commun. Theor. Phys. **39**, 433 (2003).
[29] J. S. Zhang, Commun. Theor. Phys. **39**, 83 (2003).
[30] J. S. Zhang *et al.*, Nucl. Sci. Eng. **133**, 218 (1999).
[31] X. J. Sun, J. F. Duan, J. M. Wang, and J. S. Zhang, Commun. Theor. Phys. **48**, 534 (2007).
[32] Y. L. Yan, J. F. Duan, X. J. Sun, J. M. Wang, and J. S. Zhang, Commun. Theor. Phys. **44**, 128 (2005).
[33] J. S. Zhang *et al.*, Commun. Theor. Phys. **35**, 579 (2001).
[34] J. F. Duan, Y. L. Yan, J. M. Wang, X. J. Sun, and J. S. Zhang, Commun. Theor. Phys. **44**, 701 (2005).
[35] J. F. Duan, Y. L. Yan, X. J. Sun, Y. Zhang, and J. S. Zhang, Commun. Theor. Phys. **47**, 102 (2007).
[36] W. Hauser and H. Feshbach, Phys. Rev. **87**, 366 (1952).
[37] M. Uhl, Acta Phys. **52**, 366 (1970).
[38] J. S. Zhang and X. Shi, The formulation of UNIFY code for the calculation of fast neutron data for structural materials, Report No. INDC(CPR)-014, 1989 (unpublished).
[39] C. K. Cline, Nucl. Phys. A **195**, 353 (1972).
[40] J. S. Zhang, J. M. Wang, and J. F. Duan, Commun. Theor. Phys. **47**, 1106 (2007).
[41] X. J. Sun and J. S. Zhang, Phys. Rev. C **92**, 061601(R) (2015).
[42] V. V. Verbinski and W. R. Burrus, Phys. Rev. **177**, 1671 (1969).
[43] D. R. Tilley *et al.*, Nucl. Phys. A **708**, 3 (2002).
[44] D. R. Tilley *et al.*, Nucl. Phys. A **745**, 155 (2004).